Instability of Walker Propagating Domain Wall in Magnetic Nanowires

B. Hu (胡滨) and X. R. Wang (王向荣)*
Physics Department, The Hong Kong University of Science and Technology, Clear Water Bay, Kowloon, Hong Kong and HKUST Shenzhen Research Institute, Shenzhen 518057, China
(Received 5 April 2013; published 9 July 2013)

The stability of the well-known Walker propagating domain wall (DW) solution of the Landau-Lifshitz-Gilbert equation is analytically investigated. Surprisingly, a propagating DW is always dressed with spin waves so that the Walker rigid-body propagating DW mode does not occur in reality. In the low field region only stern spin waves are emitted while both stern and bow waves are generated under high fields. In a high enough field, but below the Walker breakdown field, the Walker solution could be convective or absolute unstable if the transverse magnetic anisotropy is larger than a critical value, corresponding to a significant modification of the DW profile and DW propagating speed.

DOI: 10.1103/PhysRevLett.111.027205 PACS numbers: 75.60.Jk, 05.45.−a, 75.30.Ds, 75.60.Ch

Magnetic domain wall (DW) propagation in nanowires has attracted considerable attention in recent years [1–5] because of its fundamental interest and potential applications [2,3]. Field-driven DW dynamics is governed by the Landau-Lifshitz-Gilbert (LLG) equation which has a well-known Walker exact rigid-body propagation solution [1] for a one-dimensional (1D) biaxial wire. This Walker solution plays a pivotal role [6–8] in our current understanding of both current-driven and field-driven DW propagation in magnetic nanowires. A genuine solution of a physical system must be stable against small perturbations. Although there is no proof of the stability of the Walker solution and there are signs [9,10] that this solution may be unstable, at least under certain conditions, the validity of the Walker solution for a 1D wire is always taken as self-evident. Any deviation in experiments or numerical simulations is assumed to be attributed to the quasi-1D nature or other effects [7]. On the other hand, applications of spintronics devices require accurate description of DW motion [11–14]. Thus, the stability of the Walker propagating DW solution becomes vital in our understanding of DW propagation along a magnetic wire.

In this Letter, by using a recipe that is based on a series of recent advances in nonlinear dynamics theory, the stability of the Walker exact DW solution is theoretically analyzed. A propagating DW is always dressed with spin waves so that the Walker solution is not stable against spin-wave emission. In the low field region, only stern spin waves are emitted while both stern and bow waves emerge under high field. When the transverse magnetic anisotropy is larger than a critical value and the external field is sufficiently high, the solution is convective or absolute unstable, corresponding to severe distortion of the propagating DW profile. This shall lead to noticeable deviation of DW speed from the Walker formula besides that the DW is dressed with spin waves.

To study the stability of the Walker propagating DW solution under an external field, we consider the dimensionless 1D LLG equation [15],

$$\frac{\partial \vec{m}}{\partial t} = -\vec{m} \times \vec{h}_{\text{eff}} + \alpha \vec{m} \times \frac{\partial \vec{m}}{\partial t}. \tag{1}$$

This LLG equation describes the dynamics of magnetization $\vec{M} = \vec{m} M_s$ of a magnetic nanowire schematically shown in Fig. 1, where $\vec{m}$ is the unit direction of $\vec{M}$ and M_s is the saturation magnetization. With the easy axis along the wire ($\hat{z}$ direction) and the width and thickness being smaller than the exchange interaction length, the DW structure tends to be homogeneous in the transverse direction [16], i.e., behaves effectively 1D. We are interested in the behavior of a head-to-head DW under an external field. In Eq. (1), α is the phenomenological Gilbert damping constant. The effective field (in units of M_s) is $\vec{h}_{\text{eff}} = K_{\parallel} m_z \hat{z} - K_{\perp} m_x \hat{x} + A \partial^2 \vec{m}/\partial z^2 + H\hat{z}$, where $K_{\parallel}$, $K_{\perp}$, and A are, respectively, the easy axis anisotropy coefficient, the hard axis anisotropy coefficient, and the exchange coefficient. H is the external magnetic field parallel to $\hat{z}$. The time unit is $(\gamma M_s)^{-1}$, where γ is the gyromagnetic ratio. Using polar angle θ and azimuthal angle φ for $\vec{m}$ as shown in Fig. 1, this LLG equation has a well-known Walker propagating DW solution [1],

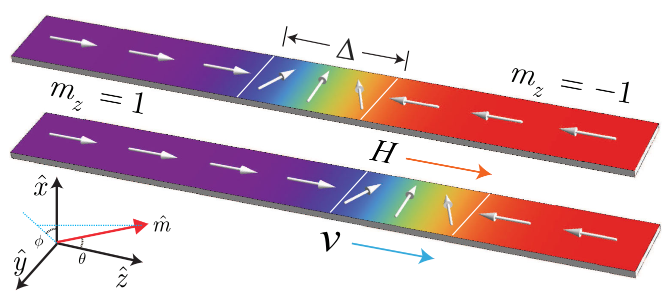

FIG. 1 (color online). Illustration of transverse head-to-head DW of width Δ in a nanowire, with easy axis along $\hat{z}$ and hard axis along $\hat{x}$. In the absence of external magnetic field (upper), a static DW exists between two domains with $m_z = \pm 1$. Under a field parallel to the easy axis, the Walker propagating DW moves towards the energy minimum state ($m_z = -1$) at a speed v while the DW profile is preserved.

$$\sin 2\varphi_w(z,t) = \frac{H}{H_c}, \qquad \ln\tan\frac{1}{2}\theta_w(z,t) = \frac{z - vt}{\Delta}. \tag{2}$$

Here $H_c = \alpha K_\perp/2$ is the Walker breakdown field and $\Delta = (K_\parallel/A + \cos^2\varphi_w K_\perp/A)^{-1/2}$ is the DW width which will be used as the length unit ($\Delta = 1$) in the analysis below. $v = \Delta H/\alpha$ is the Walker rigid-body DW speed that is linear in the external field and the DW width, and inversely proportional to the Gilbert damping constant. Solution (2) is exact for $H < H_c$.

To prove the instability of solution (2) against spin-wave emission, we follow a recently developed theory (Sandstede and Scheel [17] and Fiedler and Scheel [18]) for stability of a general traveling front such as a propagating head-to-head DW shown in Fig. 1. Consider a small deviation of the Walker solution, $\theta_w + \theta$ and $\varphi_w + \varphi$ with $|\theta| \ll 1$ and $|\varphi| \ll 1$, the equations satisfied by θ and φ can be readily obtained from Eq. (1). In the moving frame of the DW velocity v (with coordinate transformations of $z \to \xi \equiv z - vt$ and $t \to t$), the linearized equations of θ and φ in a two-component form of $\Lambda \equiv (\theta, \varphi)^T$ (superscript T means transpose) are

$$\frac{d\Lambda}{dt} = L(\theta_w, \varphi_w, \partial/\partial\xi, \partial^2/\partial^2\xi)\Lambda. \tag{3}$$

L is an inhomogeneous operator, depending on ξ through θ_w. The possible solutions of Eq. (3) of type $\Lambda = \Lambda_1(\xi)e^{\lambda t}$ define the spectrum of L. Similar to the energy spectrum of a quantum system, λ can be continuum and discrete. The former is often called an essential spectrum while the later point spectrum. The spectrum λ can tell us whether the propagating DW can destabilize the domains by emitting spin waves into them. In terms of $\Lambda' \equiv (\theta, \varphi, \partial\theta/\partial\xi, \partial\varphi/\partial\xi)^T$, Eq. (3) becomes a four-dimensional first-order ordinary differential system,

$$\frac{d}{d\xi}\Lambda' = \Gamma(\lambda)\Lambda', \qquad \Gamma(\lambda) = \begin{pmatrix} 0 & I \\ B & C \end{pmatrix}, \tag{4}$$

here I is a 2×2 identity matrix, and 2×2 matrices, B and C, have the following matrix elements: $B_{11} = \alpha\lambda/A + (1/2A)(K_\perp - 2K_\parallel - K_\perp\sqrt{1-\rho^2})\cos[2G(\xi)] - H\tanh\xi/A$, where $G(\xi)$ is the Gudermannian function and $\rho = H/H_c$; $B_{12} = (\lambda - K_\perp\rho\tanh\xi)/(A\cosh\xi)$; $B_{21} = -\cosh\xi(2\lambda + K_\perp\rho\tanh\xi)/(2A)$; $B_{22} = (\alpha\lambda - K_\perp\sqrt{1-\rho^2})/A$; $C_{11} = -v\alpha/A$; $C_{12} = -v/(A\cosh\xi)$; $C_{21} = v\cosh\xi/A$; $C_{22} = -2 - v\alpha/A$. Obviously, Eqs. (4) and (3) have the same spectrum since they are equivalent.

According to the theory of Refs. [17–21], the essential spectrum is bordered by the Fredholm borders (defined below) of (4) with Γ replaced by its two limits of $\xi \to \pm\infty$, denoted as $\Gamma^\pm \equiv \lim_{\xi\to\pm\infty}\Gamma$. Since $\Gamma^\pm$ are constant 4×4 matrices, solutions of Eq. (4) with $\Gamma = \Gamma^\pm$ are linear combinations of $\Lambda_0 e^{\kappa^\pm\xi}$ with $\kappa^\pm$ being complex numbers. Pure plane wave solutions ($\kappa^\pm = ik$) exist only when λ satisfies $\det[\Gamma^\pm(\lambda) + ik] = 0$ with $k \in (-\infty, \infty)$. Each of the two equations has two branches of allowed λ labeled as $\lambda^\pm_{1,2}(k)$, known as the Fredholm borders [17,18,20]. In other words, Eq. (4) with $\Gamma = \Gamma^+$ ($\Gamma = \Gamma^-$) has a pure plane wave solution when λ is on $\lambda^+_{1,2}(k)$ [$\lambda^-_{1,2}(k)$]. For those λ not on $\lambda^\pm_{1,2}(k)$, each Eq. (4) with $\Gamma = \Gamma^\pm$ has four $\kappa^\pm$ whose real parts are nonzero. If one uses $(n^\pm_+, n^\pm_-)$ to denote λ with $n^\pm_+$ ($n^\pm_-$) being the number of $\kappa^\pm$ with positive (negative) real part, then both $\lambda^+_{1,2}(k)$ and $\lambda^-_{1,2}(k)$ divide the λ plane into three parts with $(n^\pm_+, n^\pm_-) = (1,3)$, (2, 2), and (3, 1), respectively. According to Kato [21], the essential spectrum of L must be in the regimes with $n^+_- + n^-_+ \neq 4$. For λ on boundaries $\lambda^\pm_{1,2}$, the associated eigenmode is plane wave (spin wave) while eigenmodes for λ not on the boundaries are spin wave packets.

In order to understand the numerical results in Ref. [10], parameters of yttrium iron garnet (YIG) [14] are assumed in our analysis with $A = 3.84\times 10^{-12}$ J/m, $K_\parallel = 2\times 10^3$ J/m^3, $\gamma = 35.1$ kHz/(A/m), and $M_s = 1.94\times 10^5$ A/m. $\alpha = 0.001$ is used and $K_\perp$ is a varying parameter. Figure 2 plots the essential spectrum for $K_\perp = 1$ (in units of $\mu_0 M_s^2$ that is about 25 times larger than $K_\parallel$). In the absence of an external field, the two branches of the spectrum of $\Gamma^\pm$ are the same, $\lambda^+_{1,2}(k) = \lambda^-_{1,2}(k)$, shown in Fig. 2(a). Since the spectrum encroaches the right half plane, unstable plane waves shall exist and spin-wave emission is expected. A similar conclusion was

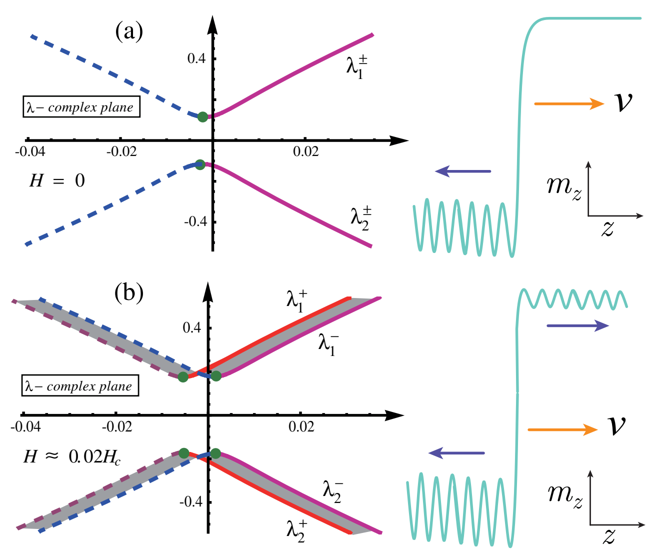

FIG. 2 (color online). Left: Essential spectrum (shadowed regions) for $H = 0$ (a) and $H \approx 0.02H_c$ (b). The Fredholm borders are $\lambda^\pm_{1,2}(k)$. Solid border lines correspond to spin waves with negative group velocities while the dashed border lines are for the spin waves with positive group velocities. Propagating DW wall emits stern waves in low fields [right of (a)], and stern and bow waves in higher field ($0.02H_c < H < H_c$) [right of (b)]. The green dots are zero group velocity modes. $K_\perp = 1$ (in units of $\mu_0 M_s^2$) is used.

also obtained in an early study [22], but for $H > H_c$. Solid lines are for negative group velocity [determined by $\mathrm{Im}(\partial\lambda/\partial k)$]; thus, these are stern modes. The dashed lines indicate positive group velocity, corresponding to bow modes. The green dots are zero group velocity points. According to Fig. 2(a), all unstable modes have negative group velocities so that DW can only emit stern waves in the low fields. As the external field increases, $\lambda^{+}_{1,2}(k)$ and $\lambda^{-}_{1,2}(k)$ will separate, and the area of essential spectrum in the λ plane becomes bigger and bigger [shadowed regimes in Fig. 2(b)]. The green dots also move toward the $\mathrm{Im}(\lambda)$ axis and cross it at $H \approx 0.02H_c$ [Fig. 2(b)]. Upon further increase of H, the unstable modes have both positive and negative group velocities although most of them have negative ones. One shall have propagating DW to emit both stern and bow waves. The stern waves should be stronger than the bow waves as schematically shown in the right-hand figure of Fig. 2(b). This is exactly what was observed in numerical simulations for stern wave emission in low field [9] and stern-and-bow wave emission in high field [10]. In a realistic wire with damping, emitted spin waves will be dissipated after a short distance and are hard to observe in experiments.

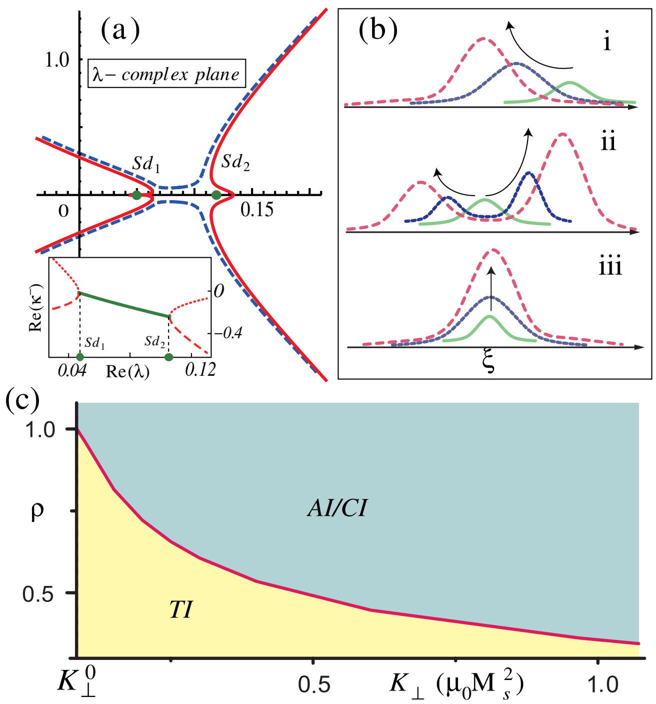

FIG. 3 (color online). (a) $\lambda^{-}_{1,2}$ for $K_\perp = 1$, $\rho = 0.35$ (dashed curve) and 0.36 (solid curve). The absolute spectrum is between two branching points Sd_1 and Sd_2 (green dots). Inset: Plot of $\mathrm{Re}(\kappa_2^-)$ (dotted curve) and $\mathrm{Re}(\kappa_3^-)$ (dashed curve) vs $\mathrm{Re}(\lambda)$ between Sd_1 and Sd_2. At $Sd_{1,2}$, $\kappa_2^- = \kappa_3^-$. (b) Graphical illustrations of three types of instabilities caused by unstable absolute spectrum. Green curves indicate initial profiles of unstable modes while the dotted (blue) and dashed (red) curves are their later profiles. A transient instability (i) emits unidirectional waves (propagating to the left). A convective instability (ii) emits waves in both directions. An absolute instability (iii) emits waves that do not travel in the moving frame, or move with the DW. (c) Phase diagram of transient (TI) and absolute or convective (AI or CI) instabilities. The boundary is the bifurcation line between AI or CI and TI instabilities in $K_\perp$ and $\rho = H/H_c$ plane. The bifurcation line is only plotted for $K_\perp \geq K_\perp^0$; here $K_\perp^0 \approx 0.085$ at which $H_2 = H_c$ ($\rho = 1$). Note that our analysis is valid for fields below the Walker breakdown value.

The essential spectrum determines the instability of domains. It says that DW propagation generates spin waves in domains separated by the DW when the essential spectrum encroaches the right half of the λ plane. Interestingly, the instability of a DW profile is determined by the so-called absolute spectrum and the branching points [17–21,23–25]. To introduce the absolute spectrum and the branching points, we recall that, for each λ in the complex plane, there are four $\kappa_i^{\pm}$ ($i = 1, 2, 3, 4$) for $\Gamma^{\pm}$ ordered by their real parts as $\mathrm{Re}(\kappa_1^{\pm}) \geq \mathrm{Re}(\kappa_2^{\pm}) \geq \mathrm{Re}(\kappa_3^{\pm}) \geq \mathrm{Re}(\kappa_4^{\pm})$. λ is said to belong to the absolute spectrum if and only if $\mathrm{Re}[\kappa_2^{+}(\lambda)] = \mathrm{Re}[\kappa_3^{+}(\lambda)]$ or $\mathrm{Re}[\kappa_2^{-}(\lambda)] = \mathrm{Re}[\kappa_3^{-}(\lambda)]$ [25,26]. The branching points are special points in the absolute spectrum, denoted as λ_{sd}, satisfying $\kappa_2^{\pm}(\lambda_{sd}) = \kappa_3^{\pm}(\lambda_{sd})$. These special points correspond also to the modes of zero group velocity, or nontraveling modes [25,26]. The instability of the absolute spectrum happens when this spectrum encroaches the right half plane, leading to severe modification of the propagating DW profile that, in turn, modifies the propagating speed [5]. In addition, if the branching point(s) also becomes unstable, then nontraveling modes will present [25,26]. For $K_\perp = 1$, the absolute spectrum in the right half λ plane is generated by Γ^-. Figure 3(a) shows two branches $\lambda^{-}_{1,2}$. They are well separated by the real axis for $\rho = 0.35$ as shown in Fig. 3(a) (dashed curves) and no absolute spectrum could be found in the right half plane. As the field increases, the two branches get closer to each other and at an onset field H_2, depending on $K_\perp$, two branches tangent at the real axis and then separate again in the horizontal direction, as shown in Fig. 3(a) for $\rho = 0.36$ (solid curves). At this moment, the absolute spectrum begins to emerge on the real axis [the segment between two branching points $Sd_{1,2}$ (green solid dots)]. The dependence of $\mathrm{Re}(\kappa_2^-)$ (dotted curve) or $\mathrm{Re}(\kappa_3^-)$ (dashed curve) on $\mathrm{Re}(\lambda)$ between these two points is shown in the inset of Fig. 3(a) (solid segment).

According to Refs. [23–25], wave packets would be emitted if the essential spectrum encroaches the right half λ plane. There are three types of instability [17–20,23–25]. The instability is called transient (TI) if the essential spectrum encroaches the right half plane and the absolute spectrum is either in the left half plane or does not exist. The propagating DW emits stern waves shown in Fig. 3(b)i. The instability is called convective if both the essential and the absolute spectrum encroach the right half

λ plane. In this case, the emitted waves can propagate in both directions as shown by Fig. 3(b)ii. For a convective instability, if any branching point is also in the right half λ plane, the instability is called absolute. An absolute instability can then emit nontraveling (zero group velocity) waves as illustrated in Fig. 3(b)iii. For the LLG equation, since the absolute spectrum is the segment connecting two branching points Sd_1 and Sd_2 [Fig. 3(a)], the absolute instability (AI) and convective instability (CI) coexist. It is known that transient instability is very weak [17,27]. Thus, we should not expect to have great physical consequences. On the other hand, the absolute instability moves with the DW, and causes the change of the DW profile [25,27,28]. It is known [5] that field-induced DW propagating speed is proportional to the energy damping rate that is sensitive to the DW profile. Therefore, absolute instability, which deforms the propagating DW profile, shall substantially alter DW speed. This may explain large deviation of DW speed from the Walker result near the breakdown field in recent simulations [10]. This deviation is subjected to experimental verification.

Figure 3(c) is the calculated phase diagram in $K_\perp$ and $\rho = H/H_c$ plane. A transition from transient instability (denoted as TI in the figure) to absolute or convective instability (AI or CI) occurs at a critical field H_2 as long as $K_\perp > K_\perp^0 \approx 0.085$ at which $H_2 = H_c$. It means no absolute or convective instability exists for $K_\perp < K_\perp^0$, and one shall not see noticeable changes in the famous Walker propagation speed mentioned early. This may explain why many previous numerical simulations on permalloy, which has small transverse magnetic anisotropy, are consistent with the Walker formula.

It should be notid that absolute or convective instability could occur as long as $K_\perp$ is above $K_\perp^0$, which is 0.085 (about twice the easy-axis anisotropy) for YIG. The value of $K_\perp^0$ depends on other model parameters. Before concluding, we would also like to point out differences between current findings and those of previous studies. Reference [22] considers the spin-wave emission effect on DW velocity above the Walker breakdown field, instead of below the breakdown field. Spin wave emission was numerically investigated in Refs. [9,10] for the zero damping case in details where, again, there is no Walker rigid-body propagation solution (breakdown field is zero). Thus, spin-wave emission is not surprising in this case because of the continuous temporal periodic deformation of DWs. To our knowledge, the only previous finding that is closer to the results reported here is the early numerical study of Ref. [10] that showed evidences of spin-wave emission near, but below, the Walker breakdown field. However, it is not clear in Ref. [10] whether spin waves could be emitted far below the Walker breakdown field. Our findings may also solve a long-term puzzle where the infinite number of propagating DWs (soliton), existing at $\alpha = 0$ and $H = 0$, are invalid when $\alpha \neq 0$ and $H \neq 0$. The answer may be that these solitons are dressed with spin waves and their analytical forms are beyond our current mathematical capability.

In conclusion, we showed that a Walker propagating DW will always emit stern waves in a low field, and both stern and bow waves in a higher field. The true propagating DW is always dressed with spin waves. The emitted spin waves shall be damped away during their propagation, making them hard to detect in realistic wires. For a realistic wire with its transverse magnetic anisotropy larger than a critical value and when the applied external field is larger than a certain value, a propagating DW may undergo simultaneous convective and absolute instabilities. As a consequence, the propagating DW will not only emit both spin waves and spin wave packets, but also change significantly its profile. Thus, the corresponding Walker DW propagating speed will deviate from its predicted value, agreeing very well with recent simulations. This finding is subjected to experimental verification.

This work is supported by Hong Kong RGC Grants No. 604109 and No. 605413 and the grant from NSF of China.

*phxwan@ust.hk

[1] N. L. Schryer and L. R. Walker, J. Appl. Phys. **45**, 5406 (1974).
[2] S. S. P. Parkin, M. Hayashi, and L. Thomas, Science **320**, 190 (2008).
[3] D. A. Allwood, G. Xiong, C. C. Faulkner, D. Atkinson, D. Petit, and R. P. Cowburn, Science **309**, 1688 (2005).
[4] G. S. D. Beach, C. Knutson, C. Nistor, M. Tsoi, and J. L. Erskine, Phys. Rev. Lett. **97**, 057203 (2006).
[5] X. R. Wang, P. Yan, J. Lu, and C. He, Ann. Phys. (Amsterdam) **324**, 1815 (2009); X. R. Wang, P. Yan, and J. Lu, Europhys. Lett. **86**, 67 001 (2009).
[6] Z. Li and S. Zhang, Phys. Rev. Lett. **92**, 207203 (2004).
[7] A. Thiaville, S. Rohart, Ju. V. Cros, and A. Fert, Europhys. Lett. **100**, 57 002 (2012).
[8] J. Linder, Phys. Rev. B **87**, 054434 (2013).
[9] R. Wieser, E. Y. Vedmedenko, and R. Wiesendanger, Phys. Rev. B **81**, 024405 (2010).
[10] X. S. Wang, P. Yan, Y. H. Shen, G. E. W. Bauer, and X. R. Wang, Phys. Rev. Lett. **109**, 167209 (2012).
[11] J. Stöhr and H. C. Siegmann, *Magnetism: From Fundamentals to Nanoscale Dynamics* (Springer-Verlag, Berlin, 2006).
[12] M. Hatami, G. E. W. Bauer, Q. Zhang, and P. J. Kelly, Phys. Rev. Lett. **99**, 066603 (2007).
[13] D. S. Han, S. K. Kim, J. Y. Lee, S. J. Hermsdoerfer, H. Schultheiss, B. Leven, and B. Hillebrands, Appl. Phys. Lett. **94**, 112502 (2009).
[14] P. Yan, X. S. Wang, and X. R. Wang, Phys. Rev. Lett. **107**, 177207 (2011).
[15] L. Landau and E. Lifshitz, Phys. Z. Sowjetunion **8**, 153 (1953); T. L. Gilbert, Phys. Rev. **100**, 1243 (1955).

[16] D. G. Porter and M. J. Donahue, J. Appl. Phys. **95**, 6729 (2004).
[17] B. Sandstede and A. Scheel, Dyn. Stab. Syst. **16**, 1 (2001); B. Sandstede and A. Scheel, Mathematische Nachrichten **232**, 39 (2001).
[18] B. Fiedler and A. Scheel, in *Trends in Nonlinear Analysis*, edited by M. Kirkilionis, S. Kromker, R. Rannacher, and F. Toni (Springer, New York, 2003).
[19] D. Henry, *Geometric Theory of Semilinear Parabolic Equations* (Springer, New York, 1981).
[20] K. J. Palmer, Proc. Am. Math. Soc. **104**, 149 (1988).
[21] L. Perko, *Differential Equations and Dynamical Systems*, (Springer, New York, 2001); T. Kato, *Perturbation Theory for Linear Operators* (Springer, New York, 1995). To understand theorem **5.35** of Chap. 4 in Kato's book that says the essential spectrum of L being in the regimes with $n_-^{\pm} + n_+^{-} \neq 4$, let us consider the case of $n_-^{\pm} + n_+^{-} > 4$. There must exist localized eigenfunction $\boldsymbol{v}$ ($\lim_{\xi \to \pm\infty} \boldsymbol{v}^{\dagger}\boldsymbol{v} = 0$) because one can find coefficients $a_i (i = 1, \ldots, n_+^{-})$ and $b_j (j = 1, \ldots, n_-^{\pm})$ such that $\boldsymbol{v} = \sum_{i=1}^{n_+^-} a_i \boldsymbol{v}_i^+$ for $\xi \leq 0$ and $\boldsymbol{v} = \sum_{j=1}^{n_-^+} b_j \boldsymbol{v}_j^-$ for $\xi \geq 0$, where $\boldsymbol{v}_i^-$ ($\boldsymbol{v}_j^+$) are the eigenstates with eigenvalues $\mathrm{Re}(\kappa_i^-) > 0$ [$\mathrm{Re}(\kappa_j^+) < 0$] in left (right) ξ axis. $\boldsymbol{v}$ must be smoothly connected at $\xi = 0$ so that $\sum_{i=1}^{n_+^-} a_i \boldsymbol{v}_i^+(\xi = 0) = \sum_{j=1}^{n_-^+} b_j \boldsymbol{v}_j^-(\xi = 0)$. There are only four (4 dimension) equations but more than four ($n_-^{\pm} + n_+^{-} > 4$) variables so that a_i and b_j exist. Furthermore, $\boldsymbol{v}$ is eigenstate of

$$\frac{d}{d\xi}\Lambda' = \Gamma^{\infty}\Lambda' \qquad \Gamma^{\infty} = \begin{cases} \Gamma^+ & \xi \geq 0 \\ \Gamma^- & \xi \leq 0. \end{cases} \tag{5}$$

Γ^{∞} is called a relatively compact perturbation to Γ. According to Kato's theorem, Γ^{∞} will not change the essential spectrum of Γ, and Eqs. (4) and (5) have identical essential spectrum.
[22] D. Bouzidi and H. Suhl, Phys. Rev. Lett. **65**, 2587 (1990).
[23] J. M. Chomaz, Phys. Rev. Lett. **69**, 1931 (1992); A. Couairon and J. M. Chomaz, Physica (Amsterdam) **108D**, 236 (1997).
[24] L. Brevdo and T. J. Bridges, Phil. Trans. R. Soc. A **354**, 1027 (1996).
[25] B. Sandstede, *Handbook of Dynamical Systems II* (North-Holland, Amsterdam, 2002); B. Sandstede and A. Scheel, Phys. Rev. E **62**, 7708 (2000).
[26] J. D. M. Rademacher, SIAM J. Appl. Dyn. Syst. **5**, 634 (2006).
[27] J. Humpherys, B. Sandstede, and K. Zumbrun, Numer. Math. **103**, 631 (2006); J. Humpherys and K. Zumbrun, Physica (Amsterdam) **220D**, 116 (2006).
[28] R. L. Pego and M. I. Weinstein, Commun. Math. Phys. **164**, 305 (1994).